Inorganic Chemistry

ARTICLE

pubs.acs.org/IC

The Étard Reaction: A DFT Study

Markus Drees[†] and Thomas Strassner*[,‡]

[†]Anorganische Chemie, Technische Universität München, Lichtenbergstrasse 4, 85747 Garching, Germany

[‡]Physikalische Organische Chemie, Technische Universität Dresden, 01062 Dresden, Germany

Supporting Information

ABSTRACT: The mechanism of the Étard reaction of chromylchloride in toluene, discovered more than a century ago, has been investigated by DFT calculations (B3LYP/6-31G(d)). The formation of the experimentally observed product can be rationalized by multiple CH-abstraction reactions.

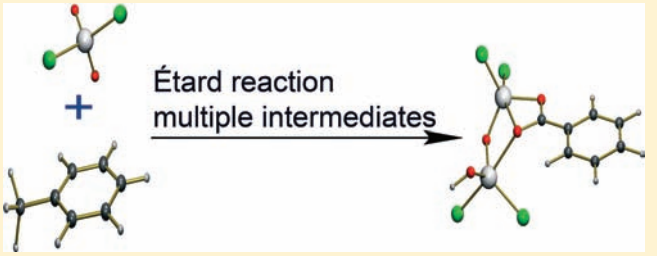

INTRODUCTION

More than 120 years ago, Étard discovered that the reaction of chromyl chloride (CrO_2Cl_2) with toluene leads to various products, e.g. benzaldehyde (32%) and benzyl alcohol (5%) together with chlorinated compounds after hydration of the initial brown precipitate.[1−4] It was proposed by Étard and generally accepted until the 1960s, that a 2:1 chromyl chloride/toluene complex ("Étard complex", Figure 1) is initially formed.[5−8] By measuring the magnetic susceptibilities Wheeler also confirmed the Cr^{IV} oxidation state which was originally proposed by Étard.[6]

Based on ESR spectra questions were raised about the structure of the complex. When Nenitzescu computed the ratio of paramagnetic chromium centers for the toluene complex from signal altitudes, this ratio was found to be 69%; e.g. 69% of the chromium atoms were found to be paramagnetic, and only 31%, diamagnetic (= Cr^{VI}).[9] These results have been questioned later on by Stairs, who concluded with the help of IR spectroscopy and new measurements of magnetic susceptibilities that all chromium atoms in the Étard complex of toluene are in the oxidation state +IV and proposed a polymeric Étard complex (Figure 2).[10]

Not only the structure of the Étard complex but also the reaction mechanism remained in the dark. More than 40 years ago Gragerov proposed a free radical process based on ESR observations,[11,12] before in the 1990s detailed kinetic studies of Mayer provided insight into the initial C−H abstraction of CrO_2Cl_2 with various hydrocarbons including toluene.[13−15] The observed product distribution based on a thorough analysis of the products is given in Figure 3. Mayer concluded that the Étard complex is not a simple stoichiometric product but an oligomeric species with the final products surrounding the chromium atoms as ligands, in agreement with the structure shown in Figure 2. The average ratio of toluene and CrO_2Cl_2 in the complex indeed was found to be 1:2.

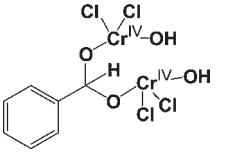

Figure 1. "Étard complex" as proposed by Étard.

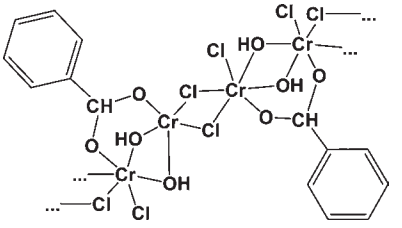

Figure 2. Polymeric Étard product.

It is interesting to note that the formation of the chlorinated product is competitive with the formation of the Étard complex, which indicates that the Étard complex might evolve via a benzyl radical which can either add a chlorine atom or a "chromyl chloride (OH) radical". The other toluene oxidation products are then obtained during workup of the Étard complex with aqueous potassium iodide solution.

Evidence for a radical mechanism comes from recent results of Cr^V as an intermediate in biochemistry and organic synthesis (oxidation of styrenes). It is well-known from experimental studies that Cr^V is the biologically active oxidation state, which

Received: April 26, 2011
Published: May 27, 2011

is responsible for the toxicity and carcinogenity of high-valent chromium(VI) compounds.[16−20]

The formation of Cr^V species in nonbiochemical systems has also been observed. We successfully synthesized Cr^V-compounds, which are 2:1-complexes of CrO_2Cl_2 and aryl-substituted alkenes. According to DFT calculations this molecular ensemble is exergonic by 41 kcal/mol compared to the starting materials.[21]

Using DFT methods Rappé calculated new pathways for the chromylchloride oxidation of alkanes as well as alkenes, which involve two metal centers.[22−24] For isobutane he suggested a high-energy intermediate generated by a C−H abstraction of CrO_2Cl_2 which can be seen as an alcohol complex at the chromium center. This complex is then trapped by another molecule chromyl chloride to form a $Cl_2OCr-O-CrOCl_2$ complex. For the Étard reaction (in toluene) this model is difficult to apply as it does not explain the experimentally observed product distribution. Only the formation of the alcohol byproduct could be explained by this mechanism, but it does not explain the formation of the halogenated carbohydrate or the main products (ketone/aldehyde). Studying the interaction of metal−oxo systems such as RuO_4 and MnO_4^- with alkanes we always observed that different spin states have to be taken into account.[25,26] From our previous experience we thought it might be possible that different spin states are also involved in the case of the Étard reaction. We present the results of a thorough density functional (DFT) study of a radical mechanism for the Étard reaction of toluene with chromyl chloride. The results of the theoretical study are in agreement with the experimental observations and the pathway previously proposed by Mayer and explain the observed products.

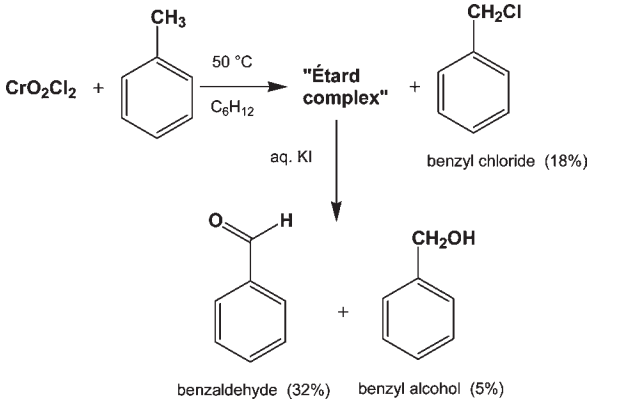

Figure 3. Products of the Étard reaction in toluene according to Mayer.[14]

COMPUTATIONAL DETAILS

All calculations were performed with Gaussian03.[27] The density functional hybrid model B3LYP[28−31] was used together with the 6-31G(d)[32−37] basis set. No symmetry or internal coordinate constraints were applied during optimizations. All reported intermediates were verified as true minima by the absence of negative eigenvalues in the vibrational frequency analysis. Transition-state structures (indicated by TS) were located using the Berny algorithm until the Hessian matrix had only one imaginary eigenvalue.[38] The identity of all transition states was confirmed by animating the negative eigenvector coordinate with MOLDEN[39] or GaussView[40] and in many cases by an IRC-calculation, given in the Supporting Information.

Approximate free energies were obtained through thermochemical analysis, using the thermal correction to Gibbs free energy as reported by Gaussian03. This takes into account zero-point effects, thermal enthalpy corrections, and entropy. All energies reported in this paper, unless otherwise noted, are free energies at standard conditions (T = 298 K, p = 1 atm), using unscaled frequencies. All transition states are saddle points on the electronic potential energy surface. The energies reported have been calculated relative to the sum of all starting materials (0 kcal/mol).

The first CH-activation via **TS1** is given relative to toluene and CrO_2Cl_2 and forms a chromium(V) species $CrO(OH)Cl_2$. During the next reaction step either the chromium(VI) species CrO_2Cl_2 or the chromium(V) species $CrO(OH)Cl_2$ can be added. For every CH-activation step we have to distinguish between these two situations which are described in detail in Schemes 1 and 2 as well as summarized in Scheme 3.

Scheme 1. $Cr^V-Cr^V-Cr^V$ Radical Pathway of the Étard Reaction of Chromylchloride with Toluene

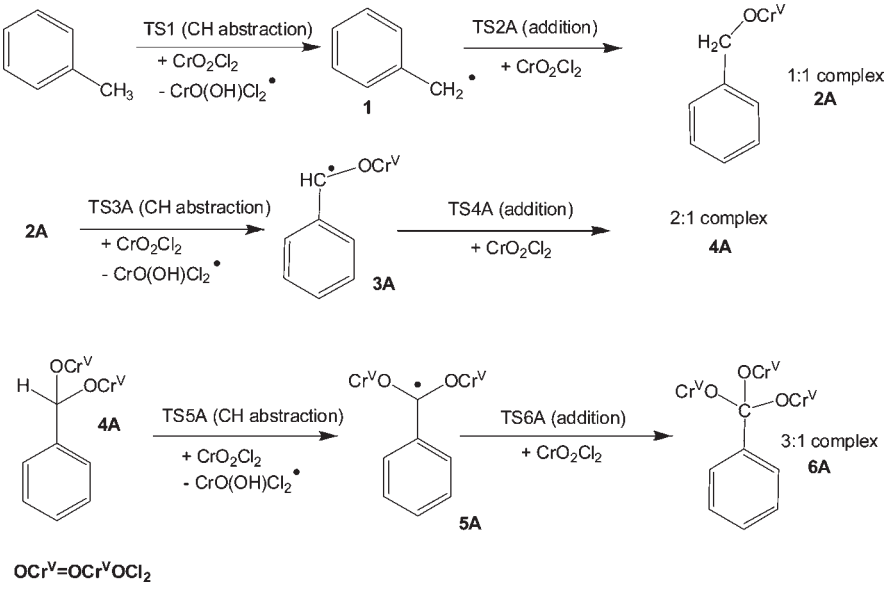

dx.doi.org/10.1021/ic200877f |Inorg. Chem. 2011, 50, 5833–5840

Scheme 2. Proposed $Cr^{IV}-Cr^{IV}-Cr^{IV}$ Radical Pathway

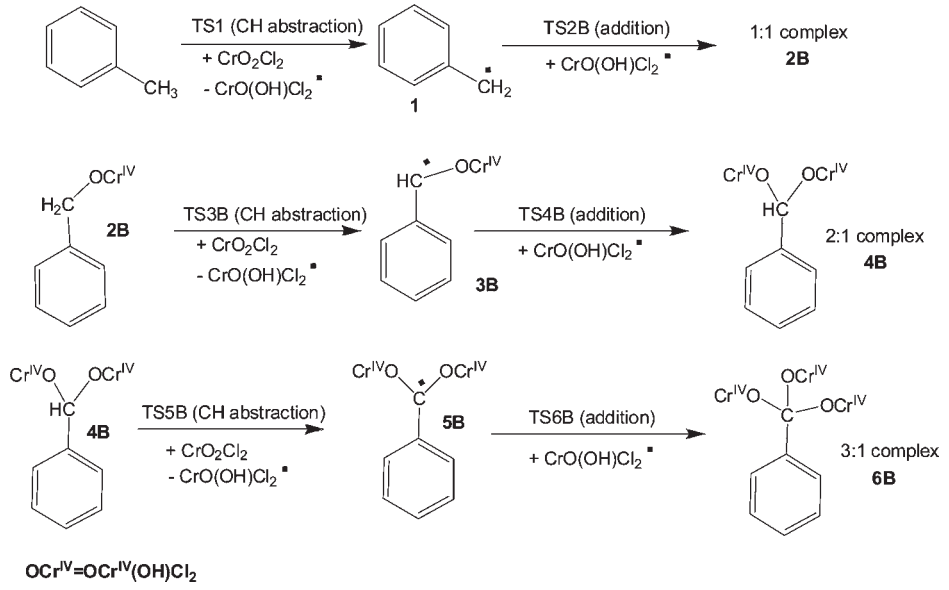

Formation of **2A** requires an additional CrO_2Cl_2; consequently, the energies given are relative to the following equation:

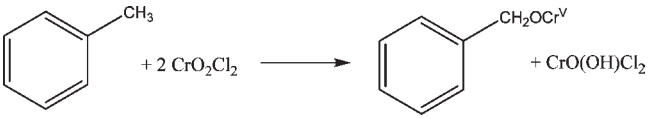

The calculated energy for the formation of **6A** (Scheme 1) is therefore given as: toluene + 6 equiv CrO_2Cl_2 → **6A** + 3 equiv $CrO(OH)Cl_2$, while **6B** is formed from toluene + 3 equiv CrO_2Cl_2 . To be able to compare the possible pathways we in every case added the corresponding starting materials; e.g. for the formation of **2A** and **2B** we used the following equations:

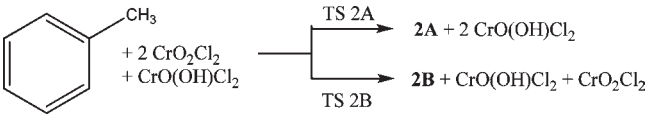

To ensure that the energy differences of all different individual steps can easily be extracted, the Supporting Information contains a table with the energies of every single step.

RESULTS AND DISCUSSION

The Radical Pathway. According to the experimental observations described in the literature, the Étard complex is expected to be a nonstoichiometric complex compound and all quantum chemical efforts to discover the appropriate mechanism have to use model systems based on experimental observations.[10,14] For the oxidation of toluene we propose a stepwise radical mechanism (Schemes 1,2). Considering that the products of the Étard reaction require multiple CH-abstractions, there have to be different pathways we need to consider. Following an initial CH-abstraction at toluene, these pathways individually consist of various CH-activation transition states, radical intermediates,

Scheme 3. Overview of All Possible Pathways Leading to the 1:1, 2:1, and 3:1 Adducts[a]

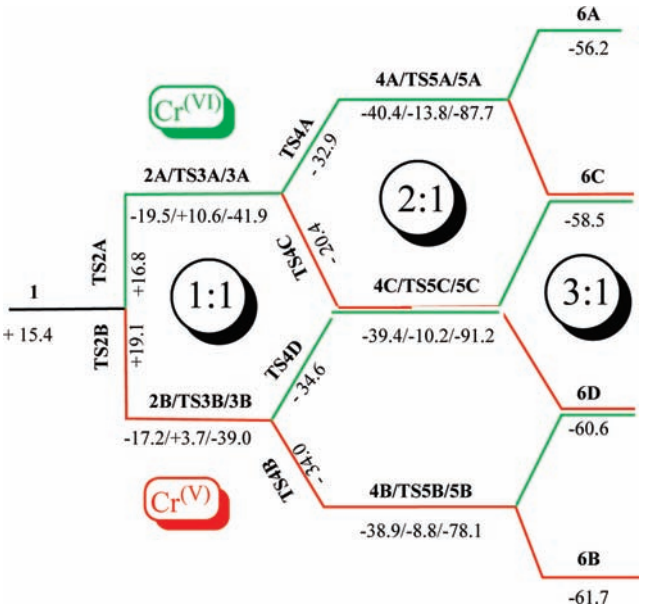

[a] Free energies are given relative to the corresponding number of chromylchlorides and toluene.

and radical addition transition states to consecutively form the 1:1 (**2**), 2:1 (**4**), and 3:1 (**6**) complexes (Scheme 3) of chromyl chloride and toluene. Only small amounts of benzoate have been observed experimentally, and most of the redox equivalents have been accounted for. Therefore, only small amounts of the 3:1 complex might have been formed. It serves as an interesting test for our calculations as they need to explain why the reaction stops after the formation of the 2:1 complex.

During the course of the radical process several different radicals can interact based on their relative energies. All possible radical reactions/combinations and additions which were considered

dx.doi.org/10.1021/ic200877f |*Inorg. Chem.* 2011, 50, 5833–5840

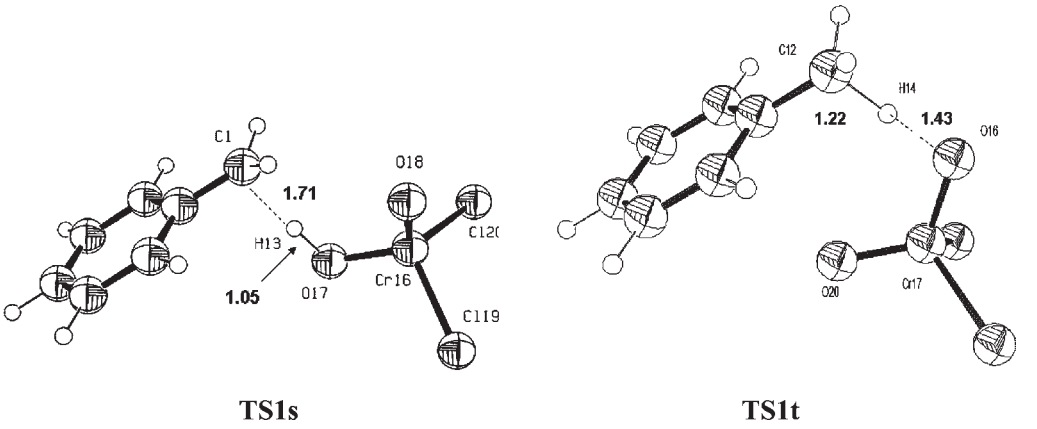

TS1s TS1t

Figure 4. Transition states of the initial C−H activation on the singlet (**TS1s**) and triplet (**TS1t**) PES.

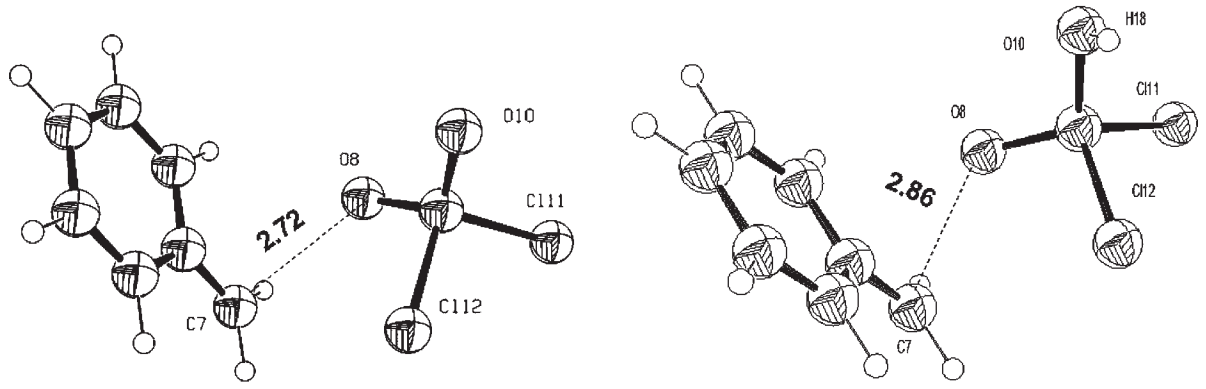

TS2A TS2B

Figure 5. Transition states for the reaction of **1** on the doublet (**TS2A**, left) and triplet surface (**TS2B**, right).

are shown in Scheme 3. To reduce the complexity the individual C−H-abstraction reactions were always calculated to be a product of the reaction of chromylchloride with the substrate, but for the addition reactions we considered Cr^{VI} (CrO_2Cl_2) as well as Cr^{V} ($CrO(OH)Cl_2$) compounds.

To make it readable we broke up the complex process into separate steps and describe them in individual schemes. The first reaction is the CH-abstraction reaction by chromyl chloride, leading to the formation of a benzyl radical and a $Cr^{V}O(OH)Cl_2$ radical. As every CH-abstraction reaction of chromylchloride produces a Cr^{V} species, the following reaction of the benzyl radical can lead to two different species. If it reacts with CrO_2Cl_2 (which is the more probable reaction, considering the excess of available chromylchloride), **2A** is formed (Scheme 1). However, in principle, also the formation of the Cr^{IV} species **2B** is possible (Scheme 2). As these possibilities exist for every CH-abstraction reaction step, Schemes 1 and 2 only show the two extreme pathways with the corresponding structures. In between these two extreme situations various other pathways could exist and lead to the 2:1 and the (nonobserved) 3:1 complexes. Scheme 3 provides the overview of all possible pathways with the corresponding calculated energies.

We first considered the initial CH-activation and found that the transition state **TS1s** (Figure 4) on the singlet potential energy surface (PES) is energetically unfavorable with $\Delta G^{\ddagger}$ = +44.2 kcal/mol ($\Delta H^{\ddagger}$ = +34.7 kcal/mol), in agreement with previous computational results,[41] but not with the experimental value determined by Mayer ($\Delta H^{\ddagger}$ = +15.5 kcal/mol, $\Delta G^{\ddagger}$ = +24.2 kcal/mol).[14]

However, the experimental results are in good agreement with the transition state **TS1t** (Figure 4) on the triplet PES. **TS1t** is an earlier transition state with a lower barrier ($\Delta G^{\ddagger}$ = +28.8 kcal/mol; $\Delta H^{\ddagger}$ = +19.0 kcal/mol) which is consistent with the change of the bond lengths of breaking (C−H) and forming (O−H) bonds. It is therefore likely that already in the first CH-abstraction a change in multiplicity of the chromylchloride from the singlet to the triplet PES occurs.

The first CH-abstraction leads to the endergonic formation of the benzyl radical **1** and the Cr^{V} species $CrO(OH)Cl_2$ (ΔG = +15.4 kcal/mol) followed by reaction of **1** with either CrO_2Cl_2 or $CrO(OH)Cl_2$ (Scheme 3), leading to the formation of two different 1:1 adducts, **2A** and **2B**.

For the corresponding transition states **TS2A** ($\Delta G^{\ddagger}$ = +1.4 kcal/mol) and **TS2B** ($\Delta G^{\ddagger}$ = +3.7 kcal/mol), shown above in Figure 5, only small barriers are calculated (Scheme S1, Supporting Information), consistent with an early transition state with long C−O bond distances between the benzyl radical carbon and the oxygen atom of the corresponding chromium−oxo species (**TS2A**: 2.72 Å/**TS2B**: 2.86 Å) The formation of the two subsequent adducts is exergonic with ΔG = −19.5 kcal/mol (**2A**) and ΔG = −17.1 kcal/mol (**2B**). We also checked **2B** on

dx.doi.org/10.1021/ic200877f |*Inorg. Chem.* 2011, 50, 5833–5840

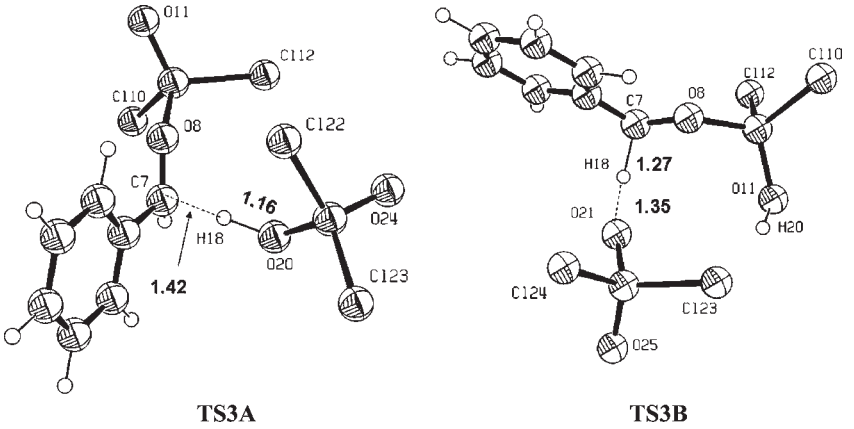

Figure 6. Transition states of the second C−H abstraction reaction on the doublet (**TS3A**) and triplet (**TS3B**) PES.

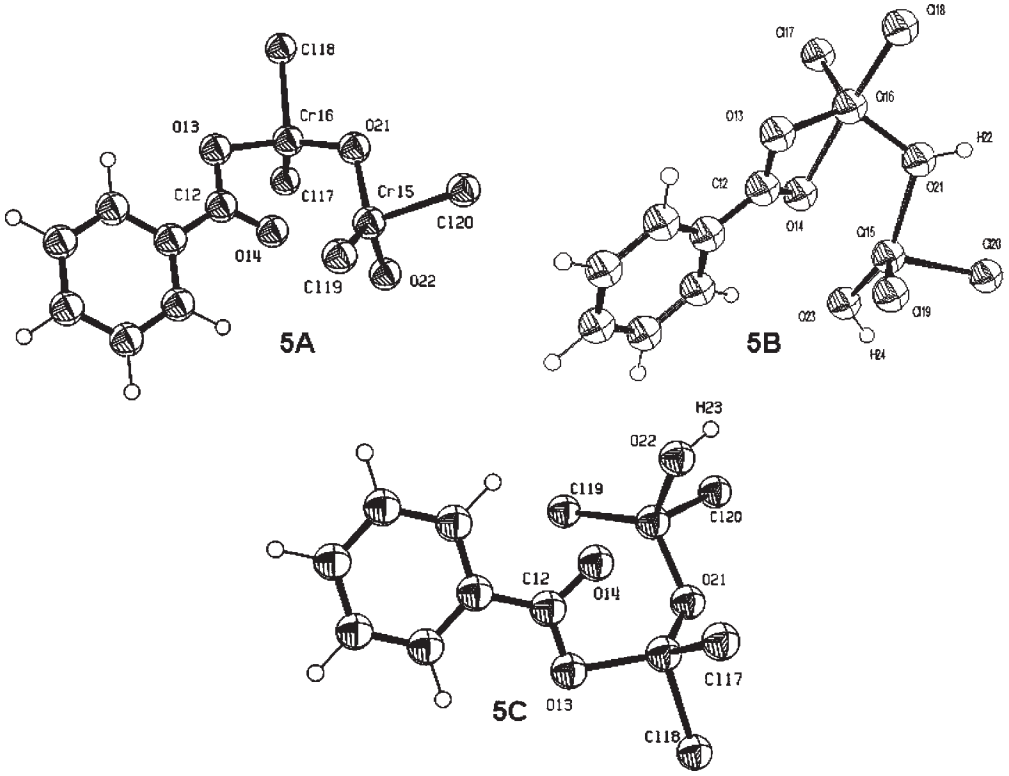

Figure 7. Products **5A**−**5C**.

the singlet surface, but it was found to be unfavorable by 34.2 kcal/mol. Structures and multiplicities are given in the Supporting Information.

The abstraction of the second hydrogen at the benzyl position requires a significantly higher activation energy of 30.1 kcal/mol (relative to **2A**) or 20.9 kcal/mol (relative to **2B**). Figure 6 shows the transition states **TS3A** ($\Delta G^{\ddagger}$ = +10.6) and **TS3B** ($\Delta G^{\ddagger}$ = +3.7), which are found on the same PES as the 1:1 complexes **2A** and **2B**. **TS3A** (on the doublet PES) is a late transition state with a C−H distance of 1.42 Å and an almost formed H−OCr bond of 1.15 Å. In contrast, for **TS3B** (on the triplet PES) both distances between C−H and H−OCr along the reaction coordinate are calculated to be 1.26 Å (Scheme S2, Supporting Information).

The second CH-abstraction leads to **3A** and **3B** which are exergonic by about 20 kcal/mol with respect to their precursors

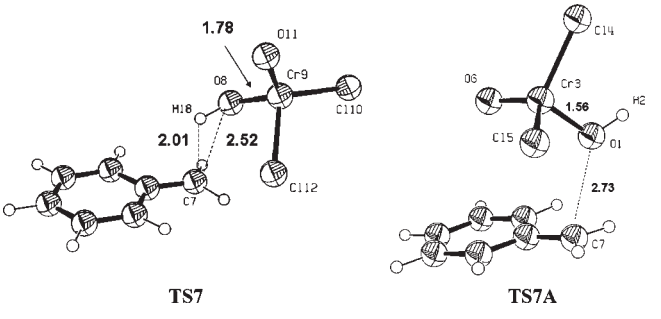

Figure 8. Structures of **TS7** and **TS7A**.

2A and **3A** and about 40 kcal/mol relative to the starting materials. Both structures show an extended planar system from

dx.doi.org/10.1021/ic200877f |*Inorg. Chem.* 2011, 50, 5833–5840

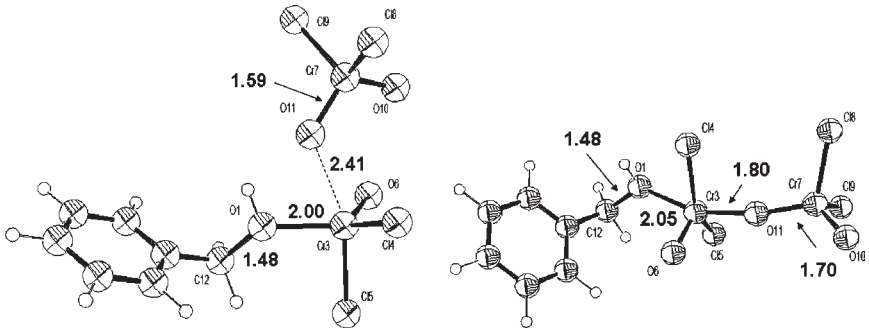

Figure 9. Structures of **TS8** (left) and the 2:1 adduct **8** (right).

the phenyl ring over the benzyl carbon atom to the oxygen atom of the metal−oxo compound. The oxygen−carbon bond lengths in both **3A** and **3B** are shortened to 1.24 Å, while the oxygen−chromium distance is elongated to 2.00 Å.

Complexes **3A** and **3B** can react with either CrO_2Cl_2 or $CrO(OH)Cl_2$, leading to four different transition states **TS4A**−**D** and three corresponding 2:1 (Étard) complexes **4A**−**C** (Scheme 2, Supporting Information). **3A** can either lead to Ph−CH-$(OCr^{V}OCl_2)_2$ (**4A**, ΔG = −40.4 kcal/mol) via **TS4A** ($\Delta G^{\ddagger}$ = −32.9 kcal/mol) with a barrier of 9.0 kcal/mol or to **4C** (ΔG = −39.4 kcal/mol) via **TS4C** ($\Delta G^{\ddagger}$ = −20.4 kcal/mol) with a higher barrier of 21.5 kcal/mol. In the case of **3B** the barriers are lower. **3B** could add $CrO(OH)Cl_2$ to form the complex Ph−CH−$(OCr^{IV}(OH)Cl_2)_2$ (**4B**, ΔG = −38.9 kcal/mol) with a barrier of 5.0 kcal/mol via **TS4B** ($\Delta G^{\ddagger}$ = −34.0) or overcome a barrier of 4.4 kcal/mol with CrO_2Cl_2 via **TS4D**.

Only for **TS4C** a larger barrier was calculated; all other transition states have small activation energies of only 5−8 kcal/mol relative to **3A** or **3B**. The relatively high activation energy of +21.5 kcal/mol (relative to **3A**) found for **TS4C** can be explained by the missing stabilizing Cr−O-interaction found in the other transition states. The corresponding products (2:1-adducts) are calculated to be endergonic by only 0.1−2.5 kcal/mol with respect to the 1:1-intermediates **3A** or **3B**.

Starting from the 2:1 species one more CH-activation could occur (Scheme S3, Supporting Information). However, the calculated activation energies for this reaction via transition states **TS5A**−**TS5C** are significantly higher compared to those of the previously discussed CH-abstraction reactions and require activation energies of about 30 kcal/mol (relative **4A**−**C**). Intermediates **5A**−**C** (Figure 7) are the most exergonic species of the different reaction pathways with calculated free energies of −78.1 to −91.2 kcal/mol (relative to all starting materials).

They are significantly more stable than the four different 3:1 complexes on the quartet (**6A**), quintet (**6C**), hextet (**6D**), and heptet (**6B**) PES. Although we tried hard, we could not find any transition state, but if we had, they would certainly be very unfavorable. Therefore, these species should not be accessible via the presented radical pathways. According to the calculations, complexes **5A**−**5C** should be the final products of these reactions, which is also in good agreement with the experimentally determined two successive "hydrogen replacement reactions"[42] and the large primary isotope effects reported by Wheeler.[43]

Are Two Metal Centers Involved? A recent investigation of the reaction of chromylchloride with isobutene proposed a reaction mechanism where two metal centers are involved in the alkane oxidation.[22,23] Although not all of the experimentally observed products of the toluene oxidation can be explained by this pathway, we looked into it as the calculated CH-activation energy for isobutene was found to be around 23 kcal/mol (depending on the functional used), similar to the energies we calculated for the pathways described above.

Rappe suggested that after an initial C−H activation by CrO_2Cl_2 a 1:1 complex is formed in a concerted fashion with $CrO(OH)Cl_2$ via the OH group at the Cr center rather than the oxo group. He reported that this pathway might decrease the barrier, but our calculations show that an analogous reaction pathway in the system CrO_2Cl_2 and toluene proceeds via a very unfavorable transition state **TS7** (Figure 8, $\Delta G^{\ddagger}$ = +41.3 kcal/mol) to form the intermediate **7**, a complex where the chromium center interacts with the toluene via the OH group (see Supporting Information).

Although we could confirm the synchronicity of the hydrogen atom transfer and an approach of the forming O−H group to the carbon atom by IRC calculations, from a thermodynamic point of view this is unlikely to be the transition state to form the 1:1 complex **7** (ΔG = −12.8 kcal/mol).

Intermediate **7** could also be formed by reaction of the benzyl radical **1** with $CrO(OH)Cl_2$ via transition state **TS7A** ($\Delta G^{\ddagger}$ = +19.7 kcal/mol) with a barrier of 4.3 kcal/mol with respect to the benzyl radical **1** and $CrO(OH)Cl_2$, where the OH group of $CrO(OH)Cl_2$ reacts with the benzyl radical. We can conclude that in the case of the toluene oxidation the formation of the 1:1-complex **7** on the triplet surface is not accessible via a concerted reaction.

A stabilizing effect was proposed for the addition of another equivalent of chromyl chloride, which forms a dimer with a Cr−O−Cr bridge.[22,23] This is also true in the toluene system, the reaction pathway on the triplet surface via the calculated barrier of +11.6 kcal/mol (**TS8**) leads to a favored 2:1 chromyl chloride dimer−benzylic alcohol complex **8** with ΔG = −16.6 kcal/mol relative to the 1:1 complex **7** (see Figure 9.

Compared to the pathways discussed above, intermediate **8** is unfavorable compared to the intermediates **2A** and **2B** and is therefore not likely to be involved. It is certainly possible that a side reaction, e.g. the formation of benzyl alcohol, which is experimentally observed in yields of about 5%, proceeds via adduct **8**, but for the general reaction we can conclude that it does not play a role.

Scheme 4 describes two possible pathways based on the data given in Scheme 3. It gives the relative energies of the lowest transition states and intermediates we calculated. The multiplicities of the pathways differ; the green line represents the pathway where the multiplicities are lower (^{2}**TS2A**, ^{2}**2A**, ^{2}**TS3A**, ^{3}**3A**, ^{3}**TS4A**, ^{3}**4A**, ^{3}**TS5A**, ^{4}**5A**) compared to the corresponding structures of

dx.doi.org/10.1021/ic200877f |*Inorg. Chem.* 2011, 50, 5833–5840

Scheme 4. Pathways Considered for the Étard Reaction: (Black) Pathway Involving Two Metal Centers (in analogy to the proposal by Rappe et al.) As Well As the Pathway to Intermediate 1; (Green) Radical Pathway, Starting at 1, Formation of 2A by Addition of CrO_2Cl_2 and Consecutive Steps towards 5A (dashed = unfeasible pathway to the 3:1 complex 6C); (Red) Pathway Starting from 1 towards 2B by Addition of $CrO(OH)Cl_2$ Continuing to 5C (dashed = unfeasible pathway to 3:1 complex 6D)[a]

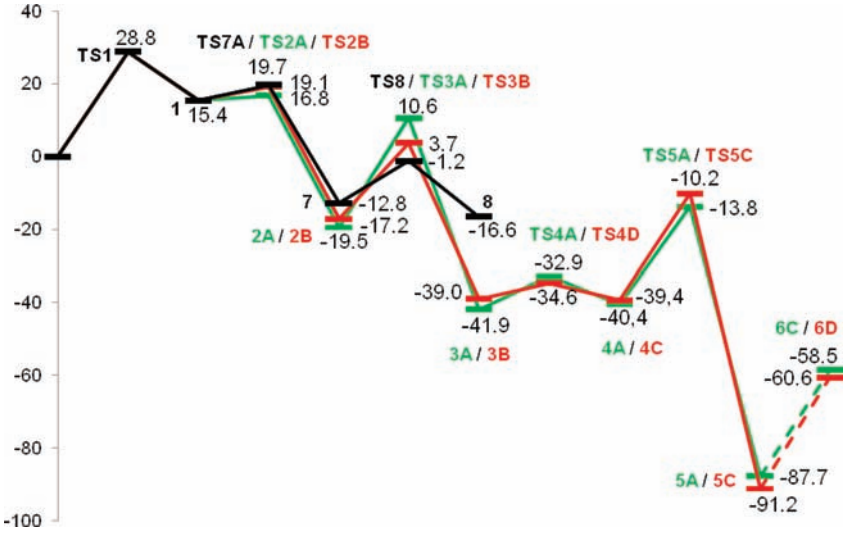

[a] All free energies given are relative to the respective equivalents of starting materials (see also Supporting Information).

the red line (^{3}**TS2B**, ^{3}**2B**, ^{3}**TS3B**, ^{4}**3B**, ^{4}**TS4D**, ^{4}**4C**, ^{4}**TS5C**, ^{5}**5C**). Pathways involving very high barriers (e.g., **TS4C**) are intentionally not included, but we added the pathway via two chromium centers (black line). Generally, the species with higher multiplicities turned out to be less favorable.

It is interesting to note that according to the computational results it would be possible to abstract also the third hydrogen atom, but the formation of any 3:1 complex is thermodynamically prohibited, in agreement with the observation of 2:1 complexes by Étard and others. These complexes can be hydrolyzed to the experimentally observed products and could also lead to the assumption of oligo- or polymerized Étard complexes as previously postulated by Stairs.[10] On the basis of the DFT results we can conclude that the Étard reaction is a complex reaction with a nonstochiometric character.

CONCLUSION

In the present work we studied the mechanism of the Étard reaction (CH-activation of toluene by chromylchloride) by density functional theory calculations. Although it is possible to cleave all three CH-bonds at toluene through a set of consecutive CH-abstraction reactions followed by different combinations of the carbon radicals with the two chromium species, CrO_2Cl_2 and $CrO(OH)Cl_2$, only two chromium molecules can add to the toluene to form a 2:1 complex, which had previously been reported in experimental papers. The results are also in agreement with kinetic and isotope effect data which indicated that two CH-activation steps are rate determining.

ASSOCIATED CONTENT

Supporting Information. This material is available free of charge via the Internet at http://pubs.acs.org.

AUTHOR INFORMATION

Corresponding Author

*E-mail: thomas.strassner@chemie.tu-dresden.de. Fax: +49 +351 4633-9679.

ACKNOWLEDGMENT

We are grateful for the computing time provided by the ZIH.

REFERENCES

(1) Étard, A. L. *C. R. Hebd. Seances Acad. Sci.* **1877**, 127–129.
(2) Étard, A. L. *C. R. Hebd. Seances Acad. Sci.* **1880**, *90*, 534.
(3) Étard, A. L. *Ann. Chim. Phys.* **1881**, *22*, 218.
(4) Étard, A. L.; Moissan, H. M. *C. R. Hebd. Seances Acad. Sci.* **1893**, *116*, 434–437.
(5) Wiberg, K. B.; Marshall, B.; Foster, G. *Tetrahedron Lett.* **1962**, 345–348.
(6) Wheeler, O. H. *Can. J. Chem.* **1960**, *38*, 2137–2142.
(7) Westheimer, F. H. *Chem. Rev.* **1949**, *45*, 419–451.
(8) Bartecki, A. *Roczniki Chemii* **1965**, *39*, 167–184.
(9) Necsoiu, I.; Balaban, A. T.; Pascaru, I.; Sliam, E.; Elian, M.; Nenitzescu, C. D. *Tetrahedron* **1963**, *19*, 1133–1142.
(10) Makhija, R. C.; Stairs, R. A. *Can. J. Chem.* **1968**, *46*, 1255–1260.
(11) Gragerov, I. P.; Ponomarchuk, M. P. *Zh. Org. Khim* **1967**, *3*, 458–464.
(12) Gragerov, I. P.; Ponomarchuk, M. P. *Zh. Org. Khim.* **1969**, *5*, 1145–1146.
(13) Cook, G. K.; Mayer, J. M. *J. Am. Chem. Soc.* **1994**, *116*, 1855–1868.
(14) Cook, G. K.; Mayer, J. M. *J. Am. Chem. Soc.* **1995**, *117*, 7139–7156.
(15) Wang, K.; Mayer, J. M. *J. Org. Chem.* **1997**, *62*, 4248–4252.
(16) Codd, R.; Dillon, C. T.; Levina, A.; Lay, P. A. *Coord. Chem. Rev.* **2001**, *216–217*, 537–582.
(17) Farrell, R. P.; Judd, R. J.; Lay, P. A.; Dixon, N. E.; Baker, R. S. U.; Bonin, A. M. *Chem. Res. Toxicol.* **1989**, *2*, 227–229.

(18) Farrell, R. P.; Lay, P. A. *Comments Inorg. Chem.* **1992**, *13*, 133–175.
(19) Levina, A.; Lay, P. A.; Dixon, N. E. *Inorg. Chem.* **2000**, *39*, 385–395.
(20) Pattison, D. I.; Lay, P. A.; Davies, M. J. *Inorg. Chem.* **2000**, *39*, 2729–2739.
(21) Strassner, T.; Mühlhofer, M.; Grasser, S. *J. Organomet. Chem.* **2001**, *641*, 121–125.
(22) Rappe, A. K. *Mol. Phys.* **2004**, *102*, 289–299.
(23) Rappe, A. K.; Jaworska, M. *J. Am. Chem. Soc.* **2003**, *125*, 13956–13957.
(24) Rappe, A. K.; Li, S. *J. Am. Chem. Soc.* **2003**, *125*, 11188–11189.
(25) Strassner, T.; Houk, K. N. *J. Am. Chem. Soc.* **2000**, *122*, 7821–7822.
(26) Drees, M.; Strassner, T. *J. Org. Chem.* **2006**, *71*, 1755–1760.
(27) Frisch, M. J.; Trucks, G. W.; Schlegel, H. B.; Scuseria, G. E.; Robb, M. A.; Cheeseman, J. R.; Montgomery, J., J. A.; Vreven, T.; Kudin, K. N.; Burant, J. C.; Millam, J. M.; Iyengar, S. S.; Tomasi, J.; Barone, V.; Mennucci, B.; Cossi, M.; Scalmani, G.; Rega, N.; Petersson, G. A.; Nakatsuji, H.; Hada, M.; Ehara, M.; Toyota, K.; Fukuda, R.; Hasegawa, J.; Ishida, M.; Nakajima, T.; Honda, Y.; Kitao, O.; Nakai, H.; Klene, M.; Li, X.; Knox, J. E.; Hratchian, H. P.; Cross, J. B.; Bakken, V.; Adamo, C.; Jaramillo, J.; Gomperts, R.; Stratmann, R. E.; Yazyev, O.; Austin, A. J.; Cammi, R.; Pomelli, C.; Ochterski, J. W.; Ayala, P. Y.; Morokuma, K.; Voth, G. A.; Salvador, P.; Dannenberg, J. J.; Zakrzewski, V. G.; Dapprich, S.; Daniels, A. D.; Strain, M. C.; Farkas, O.; Malick, D. K.; Rabuck, A. D.; Raghavachari, K.; Foresman, J. B.; Ortiz, J. V.; Cui, Q.; Baboul, A. G.; Clifford, S.; Cioslowski, J.; Stefanov, B. B.; Liu, G.; Liashenko, A.; Piskorz, P.; Komaromi, I.; Martin, R. L.; Fox, D. J.; Keith, T.; Al-Laham, M. A.; Peng, C. Y.; Nanayakkara, A.; Challacombe, M.; Gill, P. M. W.; Johnson, B.; Chen, W.; Wong, M. W.; Gonzalez, C.; Pople, J. A. *Gaussian03*; Gaussian, Inc.: Wallingford, CT, 2004.
(28) Lee, C.; Yang, W.; Parr, R. G. *Phys. Rev. B: Condens. Matter* **1988**, *37*, 785–789.
(29) Vosko, S. H.; Wilk, L.; Nusair, M. *Can. J. Phys.* **1980**, *58*, 1200–1211.
(30) Stephens, P. J.; Devlin, F. J.; Chabalowski, C. F.; Frisch, M. J. *J. Phys. Chem.* **1994**, *98*, 11623–11627.
(31) Becke, A. D. *J. Chem. Phys.* **1993**, *98*, 1372–1377.
(32) Ditchfield, R.; Hehre, W. J.; Pople, J. A. *J. Chem. Phys.* **1971**, *54*, 724–728.
(33) Hehre, W. J.; Ditchfield, R.; Pople, J. A. *J. Chem. Phys.* **1972**, *56*, 2257–2261.
(34) Hariharan, P. C.; Pople, J. A. *Chem. Phys. Lett.* **1972**, *16*, 217–219.
(35) Hariharan, P. C.; Pople, J. A. *Theor. Chim. Acta* **1973**, *28*, 213–222.
(36) Hariharan, P. C.; Pople, J. A. *Mol. Phys.* **1974**, *27*, 209–214.
(37) Rassolov, V. A.; Pople, J. A.; Ratner, M. A.; Windus, T. L. *J. Chem. Phys.* **1998**, *109*, 1223–1229.
(38) Schlegel, H. B. *J. Comput. Chem.* **1982**, *3*, 214–218.
(39) Schaftenaar, G.; Noordik, J. H. *J. Comput.-Aided Mol. Des.* **2000**, *14*, 123–134.
(40) Dennington R.,II; Keith, T.; Millam, J.; Eppinnett, K.; Hovell, W. L.; Gilliland, R. *GaussView*, 3.09 ed.; Semichem, Inc.: Shawnee Mission, KS, 2003.
(41) Tkachenko, B. A.; Shubina, T. E.; Gusev, D. V.; Gunchenko, P. A.; Yurchenko, A. G.; Schreiner, P. R.; Fokin, A. A. *Theor. Exp. Chem.* **2003**, *39*, 90–95.
(42) Stairs, R. A.; Burns, J. W. *Can. J. Chem.* **1961**, *39*, 960–964.
(43) Wheeler, O. H. *Can. J. Chem.* **1964**, *42*, 706–707.